

A two-potential formalism for the pion vector form factor

George Chanturia^{a,*}

^a*Helmholtz-Institut für Strahlen- und Kernphysik (Theorie) and Bethe Center for Theoretical Physics,
Universität Bonn, 53115 Bonn, Germany*

E-mail: g.chanturia@uni-bonn.de

We present a two-potential formalism for the pion vector form factor, which combines high-accuracy elastic phase shift data with an interaction potential between coupled channels. The model is fit to form factor data along with data from different $I = 1$ channels simultaneously. The $\pi\pi$ P-wave phase shift is used as an input. The interaction potential is composed of s -channel resonances. The results both including and excluding the input phase shift are discussed.

*RDP online PhD school and workshop “Aspects of Symmetry” (Regio2021),
8–12 November 2021
Online*

*Speaker

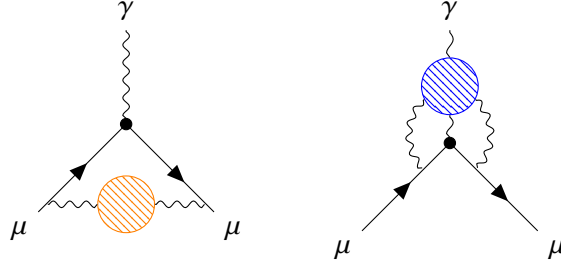


Figure 1: The hadronic vacuum polarization (left) and the hadronic light-by-light scattering (right) contributions to the anomalous magnetic moment of the muon.

1. Introduction

The pion vector form factor (VFF), defined in Eq. (1), has utmost importance in hadron physics nowadays. Perhaps the most notable significance is its relevance to the anomalous magnetic moment of the muon a_μ . The leading contributions to a_μ from the hadronic sector are the hadronic vacuum polarization (HVP) and the hadronic light-by-light scattering (HLbL) (see Fig. 1) [1]. Pions, being the lightest mesons, contribute substantially to both HVP and HLbL [2, 3]. The pion VFF gives the coupling of the pions to the electromagnetic current,

$$\langle \pi^+(q_1)\pi^-(q_2)|J^\mu|0\rangle = e(q_1 - q_2)^\mu F_V(s), \quad \text{where } s = (q_1 + q_2)^2. \quad (1)$$

Form factors are most commonly modeled by sums of Breit–Wigner functions [4] or the K-matrix formalism [5]. Since the former violates unitarity and the latter destroys analyticity, a new parametrization is needed, preserving both of these properties of the S -matrix. In this work we present such a parametrization, using a two-potential formalism, introduced in Ref. [6]. This approach has also been applied to pion and pion–kaon scalar form factors [7, 8].

2. Theory

Below the first inelastic threshold, the only allowed intermediate state is the two-pion state itself. The discontinuity of the VFF and the elastic transition matrix can be derived using the Cutkosky

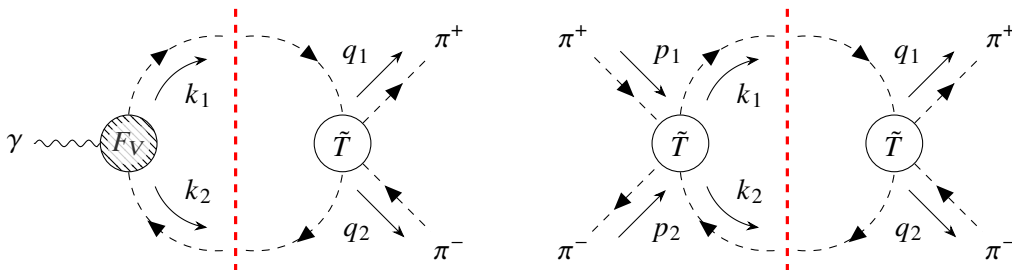


Figure 2: Cutkosky cuts due to the 2π channel for the form factor (left) and the transition matrix element (right).

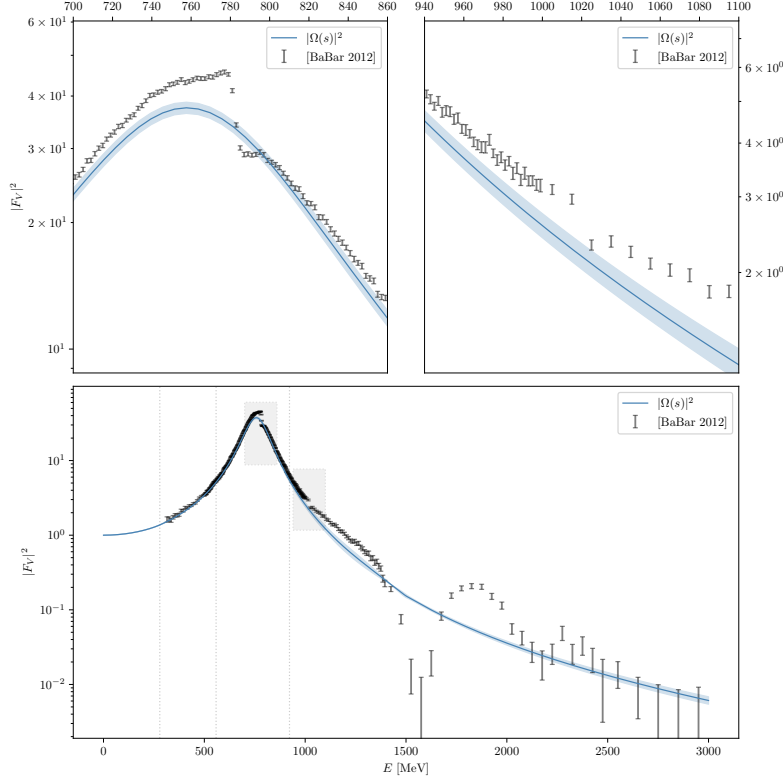


Figure 3: The Omnès solution compared to the experimental data for $F_V(s)$ from Ref. [13]. The input phase shift $\tilde{\delta}(s)$ is from Ref. [12], extrapolated to π using Eq. (4). The upper panels show the effects of $\rho - \omega$ (left) and $\rho - \phi$ (right) mixing in the data. The dotted lines denote thresholds for the $\pi\pi$, 4π , and $\pi^0\omega$ channels.

rules [9], cutting the diagrams across the intermediate states (see Fig. 2):

$$\text{disc}[F_V(s)] = 2i \text{Im}[F_V(s)] = 2i\sigma(s)\tilde{t}_1^*(s)F_V(s), \quad \text{disc}[\tilde{t}_1(s)] = 2i\sigma(s)|\tilde{t}_1(s)|^2, \quad (2)$$

where $\sigma(s) = \frac{1}{16\pi}\sqrt{1 - 4m_\pi^2/s}$ is the phase space factor for the $\pi\pi$ state. Note, how this implies $\arg \tilde{t}_1(s) = \arg F_V(s)$ [10]. Consequently, the pion VFF at low energies is driven by the $\pi\pi$ elastic scattering phase $\tilde{\delta}_1(s)$ and is given by the Omnès–Muskhelishvili solution [11]:

$$F_V(s) = \Omega[\tilde{\delta}_1](s)P_A(s), \quad \text{where} \quad \Omega[\tilde{\delta}_1](s) = \exp\left\{\frac{s}{\pi} \int_{4m_\pi^2}^{\infty} \frac{ds'}{s'} \frac{\tilde{\delta}_1(s')}{s' - s - i\epsilon}\right\}. \quad (3)$$

The $\pi\pi$ P-wave phase shift from Ref. [12] was used as the input. The input phase is valid up to $s_c = (1.5 \text{ GeV})^2$, above we have guided it smoothly to π via

$$\tilde{\delta}_1(s > s_c) = \pi + (\tilde{\delta}_1(s_c) - \pi) \left(\frac{\lambda^2 + s_c}{\lambda^2 + s} \right), \quad \text{where } \lambda = 10 \text{ GeV}. \quad (4)$$

Figure 3 shows the correspondence between the VFF data [13] and the Omnès solution. One can clearly see the $\rho(770)$ peak incorporated into the phase shift. However, the mixing effects with $\omega(782)$ and $\phi(1020)$ are not built in (see the upper two panels in Fig. 3). Apart from this, the solution clearly deviates from the data at high energies. This hints at contributions from inelastic

channels, which suggests the following strategy: we need a model that preserves both analyticity and unitarity, maps $F_V(s)$ to $\Omega[\tilde{\delta}](s)$ at low energies, provides an accurate high-energy description, and includes contributions from the coupled channels as well as isospin-violating effects such as $\rho - \omega$ and $\rho - \phi$ mixing.

3. Model

The splitting of the interaction potential has already been done in the past (see, e.g., Ref. [14]). We employ a similar procedure and split the potential into two parts [6]:

$$V_{ij}(s) = \tilde{V}_{ij}(s) + V_{Rij}(s). \quad (5)$$

$V_{ij}(s)$ is the interaction potential between channels i and j . \tilde{V} is the part coming from elastic interaction and V_R encompasses the rest. The subscript R is here to indicate that we will assume the interaction happens via s -channel resonances. By assumption, all long-ranged forces of the first channel are contained in \tilde{V} , which is purely elastic, i.e., only non-zero for $i = j = 1$. No left-hand cuts are allowed in any other channels. Accordingly, the T -matrix splits into

$$T_{ij}(s) = \tilde{T}_{ij}(s) + T_{Rij}(s), \quad (6)$$

where \tilde{T} satisfies the Lippmann–Schwinger equation: $\tilde{T} = \tilde{V} + \tilde{V}G\tilde{T}$. G denotes the propagation of the relevant channel. For instance, in the case of the $\pi\pi$ channel ($k = 1$), we have

$$G_1 = \int \frac{d^4l}{(2\pi)^4} |p_1, p_2\rangle \frac{1}{(p_1^2 - m_\pi^2 + i\epsilon)} \frac{1}{(p_2^2 - m_\pi^2 + i\epsilon)} \langle p_1, p_2|, \quad (7)$$

where p_1 and p_2 are the momenta of pions with $p_1 - p_2 = l$ and $(p_1 + p_2)^2 = s$. The vertices Γ_k are defined as

$$\begin{aligned} \Gamma_{\text{in}}^\dagger &= 1 + G\tilde{T}, & \Gamma_{\text{out}} &= 1 + \tilde{T}G, & \Gamma_1(s) &= \Omega[\tilde{\delta}_1](s); \\ \text{for other channels } (i > 1) : & & \Gamma_i(s) &= \frac{\Lambda^2}{\Lambda^2 + s}. \end{aligned} \quad (8)$$

Finally, the resonance T -matrix can be written as $T_{Rij} = \xi_i \Gamma_{\text{out},i}(t_{Rij}) \Gamma_{\text{in},j}^\dagger \xi_j$, where ξ_i denotes the centrifugal barrier factor for channel i . t_R is connected to the resonance potential via

$$t_{Rij} = V_{Rij} + V_{Rik} \underbrace{\xi_k G_k \Gamma_k \xi_k}_{\Sigma_k} t_{Rkj}, \quad t_R = [1 - V_R \Sigma]^{-1} V_R, \quad (9)$$

where the self energy Σ provides propagation of pions in the presence of elastic interaction. The discontinuity relation reads

$$\text{disc} [\Sigma_k] = \text{disc} [\xi_k G_k \Gamma_k \xi_k] = 2i\sigma_k \xi_k^2 |\Gamma_k|^2. \quad (10)$$

This allows for the integral solution

$$\Sigma_k(s) = \frac{s}{\pi} \int_{s_{\text{thr},k}}^{\infty} \frac{ds' \sigma_k(s') \xi_k^2(s') |\Gamma_k(s')|^2}{s' (s' - s - i\epsilon)}. \quad (11)$$

The subtraction constant for Σ_k is absorbed in other model parameters. Finally, the form factor can be defined as

$$\xi_i F_i = \xi_i M_i + T_{ij} G_j \xi_j M_j, \quad (12)$$

where M_k denote point-like source terms for channel k . Plugging in the T -matrix, we arrive at the final expression:

$$F_i = \Gamma_{\text{out},i} [1 - V_R \Sigma]_{ij}^{-1} M_j. \quad (13)$$

We model the resonance potential and the point-like source term as follows:

$$\begin{aligned} \bar{V}_{Rij}(s) &= - \sum_{l,l'}^{n_R} g_i^{(l)} G^{(l,l')}(s) g_j^{(l')}, & V_{Rij}(s) &= \bar{V}_{Rij}(s) - \bar{V}_{Rij}(0), \\ M_k(s) &= c_k - \sum_{l,l'}^{n_R} g_k^{(l)} G^{(l,l')}(s) \alpha^{(l')}, \end{aligned} \quad (14)$$

where n_R is the number of resonances and

$$G^{(l,l')}(s) = \frac{\delta_{l,l'}}{s - m_l^2}. \quad (15)$$

The effect of ρ mixing with ω and ϕ can be added via

$$c_1 \rightarrow c_1 \left(1 + \kappa_\omega \frac{s}{s - m_\omega^2 + im_\omega \Gamma_\omega} + \kappa_\phi \frac{s}{s - m_\phi^2 + im_\phi \Gamma_\phi} \right). \quad (16)$$

The masses $m_{\omega/\phi}$ and widths $\Gamma_{\omega/\phi}$ are taken from Ref. [15]. Note, however, that with this M_1 acquires an imaginary part and, therefore, breaks unitarity. The alternative would be to include the isospin-breaking channels into the whole picture [16]. However, we will see in the results section that this adds only a small effect (which is already clear from Fig. 3) and therefore, we follow Eq. (16) at this stage, not to complicate the fitting procedure even further. It can be shown that the effect of the resonances mixing with the photon can be added without introducing new parameters [6]. The whole list of model parameters is given in Table 1.

Parameters	Notation	Quantity
Bare masses of the resonances	m_l	n_R
Channel–resonance couplings	$g_i^{(l)}$	$n_C \times n_R$
Resonance–photon couplings	$\alpha^{(l)}$	n_R
Channel–photon couplings	c_i	$n_C - 1$
Strength parameters for ω/ϕ mixing	$\kappa_{\omega/\phi}$	2

Table 1: The list of model parameters. n_R and n_C denote the number of resonances and the number of channels respectively. Note that the amount of c_i is $n_C - 1$, since charge conservation fixes $c_1 = 1$. All parameters here are real and must be determined by the fitting procedure.

4. Application

We consider three $I = 1$ channels: $\pi\pi$, 4π , and $\pi^0\omega$ states with threshold energies equal to $2m_\pi$, $4m_\pi$, and $m_\pi + m_\omega$, respectively. The phase space and the centrifugal barrier factors for the 2-body channels are given by

$$\sigma_{ab}(s) = \frac{\sqrt{\lambda(s, m_a^2, m_b^2)}}{16\pi s}, \quad \xi_{ab}(s) = \sqrt{\frac{\lambda(s, m_a^2, m_b^2)}{3s}}, \quad (17)$$

where λ is the Källén function $\lambda(s, m_a^2, m_b^2) = (s - (m_a + m_b)^2)(s - (m_a - m_b)^2)$. This gives the expression for the cross section of e^+e^- going to channel i :

$$\sigma_{e^+e^- \rightarrow i} = \frac{e^4}{s^2} \sigma_i(s) [\xi_i(s)]^2 |F_i(s)|^2. \quad (18)$$

For the 4π channel (i.e., channel 2) we take

$$\sigma_2(s) = \frac{1}{16\pi} \left(1 - \frac{16m_\pi^2}{s}\right)^{7/2}, \quad \xi_2(s) = \sqrt{\frac{s - 16m_\pi^2}{3}}. \quad (19)$$

The vertices for all three channels are defined in Eq. (8). Λ in the vertex is not a parameter of the fit. Instead, we vary it in a certain range to obtain systematic uncertainties. For the fitting procedure we use the following data:

1. the $\pi\pi$ P-wave scattering phase: $\tilde{\delta}_1$ [3, 12, 17];
2. the vector pion form factor: F_V [13];
3. the $e^+e^- \rightarrow \pi^0\omega$ cross section: $\sigma_{e^+e^- \rightarrow \pi^0\omega}$ [18–21];
4. the $\pi\pi$ elasticity parameter: η_1 [22];
5. the non- 2π over 2π cross section ratio: r [23].

5. Results

5.1 Input Phase + Resonance Potential

We have fitted the model with 3 channels (enlisted above) and 3 resonances. The resulting curves for the $\pi\pi$ and the $\pi^0\omega$ form factors are shown in Fig. 4. As one can clearly see from the plots, we have not been able to reconstruct the $\rho(770)$ peak in the $\pi^0\omega$ form factor. The reason is that the ρ peak enters the picture through the self-energy of the $\pi\pi$ channel and the resonance potential is not strong enough at low energies to couple the $\pi\pi$ and $\pi^0\omega$ channels to each other. The resulting parameters are given in Table 2. For this fit we have ignored the r data set. The current model strongly exploits the 4π channel for the width generation of the resonances, which made us unable to do the simultaneous fit to the r value. This needs to be improved in future procedures.

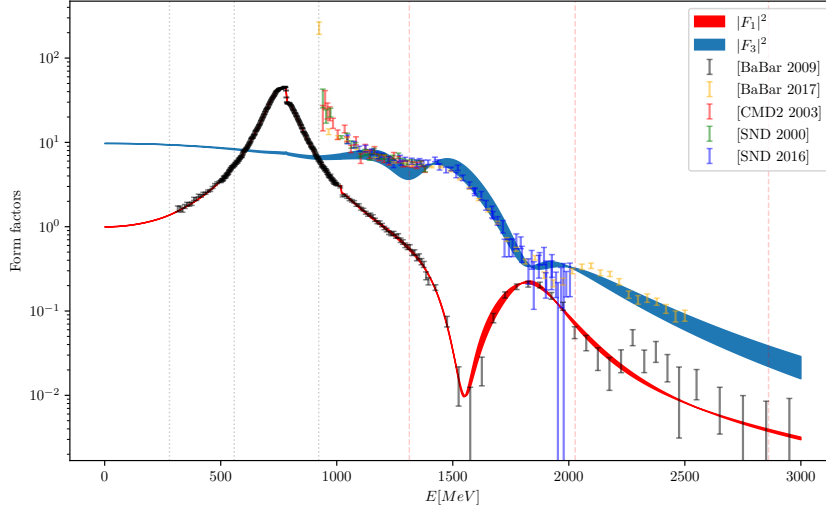


Figure 4: Fit #1: results for 3 channels and 3 resonances. Form factors for the $\pi\pi$ (red) and the $\pi^0\omega$ channel (blue) compared with the data. Dotted gray vertical lines are threshold energies and dashed red vertical lines are the masses of resonances. The indicated uncertainties are due to the value of Λ , which we vary in the range from 4 GeV to 7 GeV.

5.2 Resonance Potential

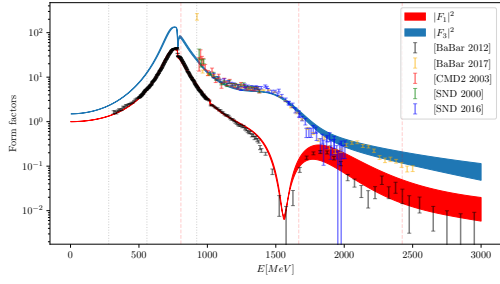
For the second fit we have removed the input phase from the model, which effectively leaves us with only the resonance potential (again, we fit 3 resonances). The idea was to include the $\rho(770)$ not through the input phase shift but as a resonance of the model. This way the ρ couples directly to the

$m_1 = 1313 \pm 13 \text{ MeV}$	$m_2 = 2027 \pm 27 \text{ MeV}$	$m_3 = 2860 \pm 51 \text{ MeV}$
$g_{11} = -0.07 \pm 0.03$	$g_{12} = -5.33 \pm 0.19$	$g_{13} = 1.67 \pm 0.13$
$g_{21} = 0.12 \pm 0.48$	$g_{22} = 2.89 \pm 0.16$	$g_{23} = 25.0 \pm 1.5$
$g_{31} = -4.85 \pm 0.63$	$g_{32} = -24.0 \pm 0.07$	$g_{33} = -8.75 \pm 1.2$
$\alpha_1 = -0.56 \pm 0.01$	$\alpha_2 = -0.002 \pm 0.007$	$\alpha_3 = -0.14 \pm 0.03$
$c_2 = 12.9 \pm 1.0$	$c_3 = 3.13 \pm 0.25$	
$\kappa_\omega = -0.002 \pm 0.0008$	$\kappa_\phi = 0.0005 \pm 0.0024$	

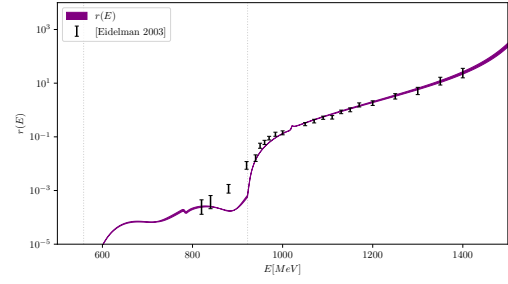
Table 2: Results of the fit #1: $\chi^2/\text{d.o.f.} = 3.13$ (excluding the r data set).

$m_1 = 806 \pm 2 \text{ MeV}$	$m_2 = 1667 \pm 23 \text{ MeV}$	$m_3 = 2423 \pm 36 \text{ MeV}$
$g_{11} = -6.0 \pm 0.3$	$g_{12} = -0.53 \pm 0.17$	$g_{13} = 1.59 \pm 0.22$
$g_{21} = -0.50 \pm 0.07$	$g_{22} = -4.11 \pm 0.07$	$g_{23} = -7.73 \pm 0.27$
$g_{31} = 4.29 \pm 0.32$	$g_{32} = -24.5 \pm 1.1$	$g_{33} = -24.8 \pm 1.4$
$\alpha_1 = -0.47 \pm 0.02$	$\alpha_2 = -0.343 \pm 0.004$	$\alpha_3 = 0.13 \pm 0.01$
$c_2 = -1.2 \pm 2$	$c_3 = 1.22 \pm 0.16$	
$\kappa_\omega = 0.020 \pm 0.009$	$\kappa_\phi = 0.001 \pm 0.004$	

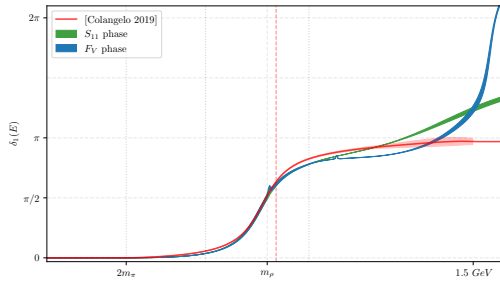
Table 3: Results of the fit #2: $\chi^2/\text{d.o.f.} = 5.05$ excluding the $\tilde{\delta}_1$ data set and 88.32 including it.



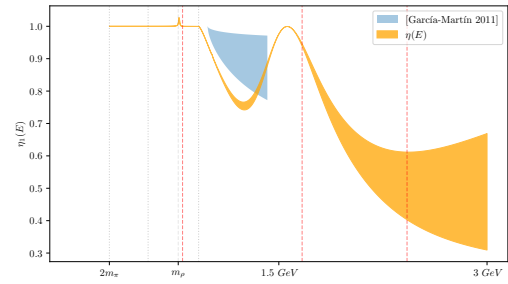
(a) Form factors for the $\pi\pi$ (red) and the $\pi^0\omega$ (blue) channel compared with the data.



(b) The non- 2π to 2π cross section ratio compared with the data from Ref. [23].



(c) The scattering (green) and the form factor (blue) phases compared to δ_1 from Ref. [3] (red).



(d) Elasticity parameter η_1 (yellow) compared to the parametrization given in Ref. [22] (light blue).

Figure 5: Fit #2: results for 3 channels and 3 resonances. Dotted gray vertical lines are threshold energies and dashed red vertical lines are the masses of resonances. The indicated uncertainties are due to the value of Λ , which we vary in the range from 4 GeV to 7 GeV.

$\pi^0\omega$ channel and the difficulty of the reconstruction of its signal in F_3 would be resolved. The fitting results are shown in Fig. 5 and the parameters are listed in Table 3. One can clearly see the $\rho(770)$ peak in both $\pi\pi$ and $\pi^0\omega$ form factors now. Moreover, the r ratio, which contains the information about the 4π channel, is also reproduced more accurately. The shortcoming of the fit, however, lies within the phase shifts. Since we do not have an input phase, the scattering phase is reconstructed from the resonance potential. Due to the exceptional precision of the Bern phase shifts, including the data set increases the χ^2 value tremendously (see the comparison within the caption of Table 3). We deduce therefrom that the resonance model is far too simple compared with the methods used in Refs. [3, 12] to reconstruct the scattering phase accurately (for instance, the model completely ignores left-hand cuts for the moment, which are crucial to describe $\pi\pi$ scattering).

6. Conclusions

We have used two different approaches to describe the data for the pion VFF and the $\pi^0\omega$ production form factor simultaneously. Within the first approach we have combined the high precision $\pi\pi$ P-wave phase shifts with a resonance potential in a way that preserves unitarity and analyticity. We have found that the resonance potential alone is not strong enough to reconstruct the $\rho(770)$ peak

in the $\pi^0\omega$ channel. This could be improved adding a contact interaction between the channels. In addition, including the $\omega \rightarrow \pi^0\gamma^*$ decay data to the fit could lead to further improvements.

Our second strategy was to use a simple resonance model without the input phase shift, employing a unitarized Gounaris–Sakurai model. The results of the fit show that both $\pi\pi$ and $\pi^0\omega$ form factors can be described within the unified resonance model. However, the simplicity of the model renders the resulting phase shifts incompatible with the results of much more involved research from the past. This problem could also be dealt with by keeping the input phase and introducing a contact interaction.

The predicted cross-section ratio r deviates from the experimental values between the 4π and $\pi^0\omega$ thresholds. This discrepancy could be improved by adding exclusive 4π data into the fitting procedure. The analysis could be improved with the ongoing research of the amplitude of the reaction $e^+e^- \rightarrow 4\pi$. In particular, the $a_1\pi$ intermediate state could be included into the model (for the role of $a_1(1260)$ in the 4π processes see, e.g., Refs. [24, 25]). We leave such improvements to future research.

Acknowledgments

I want to thank Christoph Hanhart and Bastian Kubis for supervising this project. The research was partially funded by the Volkswagenstiftung (Grant No. 93562).

References

- [1] T. Aoyama, N. Asmussen, M. Benayoun, J. Bijnens, T. Blum, M. Bruno et al., *The anomalous magnetic moment of the muon in the Standard Model*, *Physics Reports* **887** (2020) 1166.
- [2] G. Colangelo, M. Hoferichter, M. Procura and P. Stoffer, *Dispersion relation for hadronic light-by-light scattering: two-pion contributions*, *Journal of High Energy Physics* **2017** (2017) 161.
- [3] G. Colangelo, M. Hoferichter and P. Stoffer, *Two-pion contribution to hadronic vacuum polarization*, *Journal of High Energy Physics* **2019** (2019) 6.
- [4] G.J. Gounaris and J.J. Sakurai, *Finite-width corrections to the vector-meson-dominance prediction for $\rho \rightarrow e^+e^-$* , *Phys. Rev. Lett.* **21** (1968) 244.
- [5] R.H. Dalitz, *On the strong interactions of the strange particles*, *Rev. Mod. Phys.* **33** (1961) 471.
- [6] C. Hanhart, *A new parameterization for the pion vector form factor*, *Physics Letters B* **715** (2012) 170177.
- [7] S. Ropertz, C. Hanhart and B. Kubis, *A new parametrization for the scalar pion form factors*, *The European Physical Journal C* **78** (2018) 1000.
- [8] L. von Detten, F. Noël, C. Hanhart, M. Hoferichter and B. Kubis, *On the scalar πK form factor beyond the elastic region*, *The European Physical Journal C* **81** (2021) 420.

- [9] R.E. Cutkosky, *Singularities and discontinuities of Feynman amplitudes*, *Journal of Mathematical Physics* **1** (1960) 429.
- [10] K.M. Watson, *Some general relations between the photoproduction and scattering of π mesons*, *Phys. Rev.* **95** (1954) 228.
- [11] R. Omnès, *On the Solution of certain singular integral equations of quantum field theory*, *Nuovo Cim.* **8** (1958) 316.
- [12] I. Caprini, G. Colangelo and H. Leutwyler, *Regge analysis of the $\pi\pi$ scattering amplitude*, *The European Physical Journal C* **72** (2012) 1860.
- [13] BaBaR, *Precise measurement of the $e^+e^- \rightarrow \pi^+\pi^-(\gamma)$ cross section with the initial-state radiation method at BABAR*, *Physical Review D* **86** (2012) 032013.
- [14] K. Nakano, *Two-potential formalisms and the Coulomb–nuclear interference*, *Phys. Rev. C* **26** (1982) 1123.
- [15] PARTICLE DATA GROUP collaboration, *Review of Particle Physics*, *PTEP* **2020** (2020) 083C01.
- [16] S. Holz, C. Hanhart, M. Hoferichter and B. Kubis, *A dispersive analysis of $\eta' \rightarrow \pi^+\pi^-\gamma$ and $\eta' \rightarrow \ell^+\ell^-\gamma$* , 2202.05846.
- [17] G. Colangelo, J. Gasser and H. Leutwyler, *$\pi\pi$ scattering*, *Nuclear Physics B* **603** (2001) 125179.
- [18] BaBaR, *Measurement of the $e^+e^- \rightarrow \pi^+\pi^-\pi^0\pi^0$ cross section using initial-state radiation at BABAR*, *Physical Review D* **96** (2017) 092009.
- [19] CMD-2, *Study of the process $e^+e^- \rightarrow \omega\pi^0 \rightarrow \pi^0\pi^0\gamma$ in c.m. energy range 9201380 MeV at CMD-2*, *Physics Letters B* **562** (2003) 173181.
- [20] SND, *The process $e^+e^- \rightarrow \omega\pi^0 \rightarrow \pi^0\pi^0\gamma$ up to 1.4 GeV*, *Physics Letters B* **486** (2000) 2934.
- [21] SND, *Updated measurement of the $e^+e^- \rightarrow \omega\pi^0 \rightarrow \pi^0\pi^0\gamma$ cross section with the SND detector*, *Physical Review D* **94** (2016) 112001.
- [22] R. García-Martín, R. Kamiski, J.R. Peláez, J. Ruiz de Elvira and F.J. Ynduráin, *Pion–pion scattering amplitude. IV. Improved analysis with once subtracted Roy-like equations up to 1100 MeV*, *Physical Review D* **83** (2011) 074004.
- [23] S. Eidelman and L. Łukaszuk, *Pion form factor phase, $\pi\pi$ elasticity and new e^+e^- data*, *Physics Letters B* **582** (2004) 2731.
- [24] CMD-2 collaboration, *$a_1(1260)\pi$ dominance in the process $e^+e^- \rightarrow 4\pi$ at energies 1.05 GeV – 1.38 GeV*, *Phys. Lett. B* **466** (1999) 392.
- [25] A. Bondar, S. Eidelman, A. Milstein and N. Root, *On the role of the $a_1(1260)$ meson in $\tau \rightarrow 4\pi\nu_\tau$ decay*, *Physics Letters B* **466** (1999) 403407.